Structural Characterization of Erbium-doped Zinc Tellurite Glass Modified with Antimony Oxide Towards the Development of Materials for Optical Amplifier

Muhammad Hazmi Che Ku Abu **Bakar**[1], Hafizah Noor **Isa**[1*]

[1]Department of Physics, Kulliyyah of Science, International Islamic University Malaysia, Jalan Sultan Ahmad Shah, 25200 Kuantan, Pahang, Malaysia.

*Corresponding author's phone: +60 18-988 4407
E-mail: hafizahnoorisa@iium.edu.my

Received: 10 September 2025; Accepted:13 October 2025

ABSTRACT

Tellurite (TeO_2) glass has attracted significant attention in nanomaterial research due to its high solubility of rare-earth doping, making them as promising host materials for rare earth ion doping like erbium (Er^{3+}). These properties are mainly due to its structural feature that contains lone pair electron (LPE) within TeO_2 structural units which contributes to the linear and non-linear optical properties. Notably, with these properties, Er^{3+}-doped TeO_2 glass has the potential application in optical amplifier. However, the presence of this LPE also prevent TeO_2 to form a stable glass on its own under conventional melt quenching method. In this study, we show that the addition of modifiers like zinc oxide (ZnO) and a small concentration of antimony oxide (Sb_2O_3) can enhance the network stability of TeO_2 glass as well as improving its properties. A series of 60 TeO_2 – 40 ZnO – xSb_2O_3 – yEr_2O_3 ($0 < x < 1$ mol%, $0 < y < 3$ mol%) glasses were synthesized using melt quenching technique under controlled parameter, and the structural properties of the glasses were investigated using x-ray diffraction (XRD) analysis and Fourier transform infrared (FTIR) spectroscopy. XRD analysis shows no crystalline peak, revealing the amorphous structure for all samples. The FTIR spectra show the strong absorption at 690 cm^{-1} for all samples, indicating the TeO_3-rich environment in the glass network due to the high concentration of ZnO. The addition of Sb_2O_3 and Er_2O_3 alters the short-range structural environment in TeO_2 glass mostly on the TeO_3 unit as observed in the shifting in the region 700 – 800 cm^{-1}. Our findings show that these structural modifications can heavily impact optical properties such as the absorption and luminescence which could mostly be desired for optical and photonics applications like optical amplifiers. Future study can be done to explore its optical performance, such as the absorption, emission spectra, and fluorescence lifetime measurements, to evaluate their effectiveness as rare-earth-doped materials for optics and photonics application.

Keywords— Tellurite glass; rare-earth; FTIR spectroscopy; XRD analysis; and optical amplifier

1.0 INTRODUCTION

Recently, the studies of rare-earth ions doping have attracted various attentions from the researchers because of its frequent utilisation to improve the physical and optical properties of the glass host [1]. Among these rare-earth ions, erbium ion (Er^{3+}) possesses efficient broadband emission and can amplify light at 1.53 μm, a key wavelength in fibre optics [2]. Notably, with these properties, Er^{3+}-doped glass has potential applications in optical amplifiers. To achieve the full potential of Er^{3+} doping, a suitable host material is needed to ensure efficient luminescence and minimal non-radiative losses. The host material should possess low phonon energy, high rare-earth

solubility, and good thermal and chemical stability to help maintain the emission efficiency of Er^{3+} ions. For the past years, researchers have used oxide glasses because of their high chemical durability, thermal stability, and excellent insulating and optical properties, which make them suitable to be utilised as host materials for rare-earth doping. Nonetheless, there are challenges remaining in identifying a suitable combination of oxides as host systems that can balance glass-forming ability with desirable optical performance. This study focuses on Er^{3+}-doped zinc tellurite glasses modified with antimony(III) oxide (Sb_2O_3), aiming to address these challenges and explore their structural suitability for optical amplifier applications.

2.0 THEORY/LITERATURE REVIEW

Tellurite (TeO_2) glass has been widely investigated for its unique optical properties, such as broad transmission range around 0.4 to 6 μm, high nonlinear refractive index, and low phonon energies between 700 and 900 cm^{-1} [3]. In addition, TeO_2-based glass also possesses a high solubility for rare-earth ions, which makes it a promising candidate for a host material for rare-earth doping [4]. However, it is difficult to prepare TeO_2 glass under the conventional melt quenching technique [5]. The configuration of TeO_2 glass is similar to TeO_2 crystal, which makes the network structure of TeO_2 highly compact and rigid. This makes TeO_2 favour crystallisation during the quenching process. To bypass crystallisation, TeO_2 needs to be quenched at an exceedingly high rate [6]. An easier way to fabricate TeO_2 glass through melt quenching is by adding the other oxides like zinc oxide (ZnO) and antimony(III) oxide (Sb_2O_3) into TeO_2 glass to promote its glass-forming ability [7]. ZnO can reduce the rigidity of the TeO_2 glass network by transforming the high coordination of the TeO_4 trigonal bipyramidal (tbp) unit into a lower coordination unit like TeO_3 trigonal pyramid (tp) unit, which is less rigid [8]. Zinc tellurite glass shows great potential for optical properties due to its high refractive index, wide transmission window, and non-linear optical behaviour [9], [10]. In addition, Sb_2O_3 is known as a glass stabiliser and a source of non-linear optical properties, such as high non-linear refractive index [11]. Sb_2O_3 can also act as both network formers and network modifiers, depending on their coordination environment [12]. Therefore, the inclusion of ZnO and Sb_2O_3 plays a significant role in altering the fundamental structural units of TeO_2 glass.

In terms of oxygen bonding, TeO_4 units are generally associated with bridging oxygen (BO), while TeO_3 units are linked to non-bridging oxygen (NBO) [13]. The conversion of TeO_4 to TeO_3 upon the addition of modifiers is crucial as the presence of BO and NBO in the glass is a key structural change that directly influences the optical properties of TeO_2-based glasses. Hence, to observe the ratio of BO and NBO within the glass structure, Fourier Transform Infrared (FTIR) spectroscopy is employed as it is a suitable method to detect the vibration modes associated with BO and NBO in TeO_2 glass. FTIR is chosen for its effectiveness in detecting the vibrational modes in the bonds, such as the stretching and bending vibration in distinctive structural groups that represent the glass matrix [14]. In this study, the FTIR spectroscopy was used to analyse the structural characteristics of Er^{3+}-doped zinc tellurite glass by identifying the vibrational modes of the chemical bonds within the glass network. The identification helps to determine the structural evolution of TeO_2 glass with the addition of the modifiers, such as ZnO, Er_2O_3 and Sb_2O_3.

3.0 MATERIALS

Tellurium dioxide (>99.5%), zinc oxide (99.9%), antimony(III) oxide (99.999%), and erbium(III) oxide (99.9%) were purchased from Sigma Aldrich.

4.0 EXPERIMENTAL

A series of TeO_2 – ZnO – Sb_2O_3 – Er_2O_3 glasses were synthesized via melt quenching technique by varying the composition of the materials using the stoichiometric formula (60.0 − x − y) TeO_2 – 40.0 ZnO – x Sb_2O_3 – y Er_2O_3, where x = 0, 0.5, and 1.0 mol %, and y = 0, 1.5, 3.0, and 5.0 mol %. A total of 6 glass samples were prepared, and the composition of each sample was tabulated in Table 1. The required amount of tellurium dioxide (TeO_2), zinc oxide (ZnO), antimony(III) oxide (Sb_2O_3), and erbium(III) oxide (Er_2O_3) were calculated and weighed accordingly using a digital weight machine at a total of ~6 g. The powders were weighed and mixed homogeneously, transferred into an alumina crucible, and placed inside the furnace for the preheating process at 400 °C for 2 hours. After 2 hours, the crucible was transferred into another furnace for the melting process at 1100 °C for 1 hour. Then, the melted sample was cast on the preheated brass plate and annealed in the first furnace at 370 °C for 2 hours to remove the thermal stress that can cause the glass to develop cracks. Finally, the furnace is turned off to let the sample slowly cool to room temperature.

TABLE 1: Molar compositions of the glass material

Sample annotation	Molar percentage of the glass material (mol %)			
	TeO_2	ZnO	Sb_2O_3	Er_2O_3
S1	57.0	40.0	0.0	3.0
S2	55.0	40.0	0.0	5.0
S3	56.5	40.0	0.5	3.0
S4	56.0	40.0	1.0	3.0
S5	59.5	40.0	0.5	0.0
S6	58.0	40.0	0.5	1.5

The structural properties of the glasses were assessed using x-ray diffractometer to determine their amorphous nature and Fourier Transform Infrared (FTIR) spectroscopy for the detection of functional groups in the glass network. The glasses were ground into a powder form and examined using Bruker D8 Advance x-ray diffractometer. The x-ray diffraction (XRD) analysis was carried out with CuK_α radiation source of wavelength λ = 1.5406 Å at the range 2θ between 10° to 80°. For FTIR analysis, the spectra were recorded using PerkinElmer Frontier FT-IR. The KBr pellet technique was employed, and the analysis was carried out in the range of 400 – 4000 cm^{-1}. All the measurements were done at the resolution of 4.0 cm^{-1}.

5.0 RESULTS AND DISCUSSION

5.1 X-Ray Diffraction (XRD)

Fig. 1 shows the x-ray diffraction (XRD) spectra of the glasses that were scanned from 10° to 80° of 2θ. It is observed that there are no visible sharp peaks, which indicates the properties of the amorphous structure. There were observable broad humps at 20° to 35° for all samples, which indicate the short-range order in the glass network [15]. From the XRD spectra, it can be concluded that amorphous Er^{3+}-doped zinc tellurite glasses modified with Sb_2O_3 have been successfully prepared via the melt quenching technique.

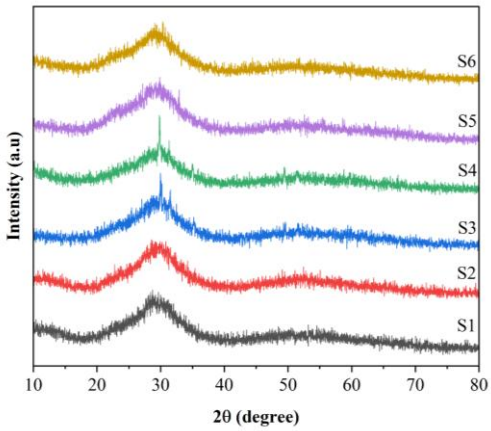

Fig. 1: XRD spectra of Er^{3+}-doped zinc tellurite glasses series at various compositions.

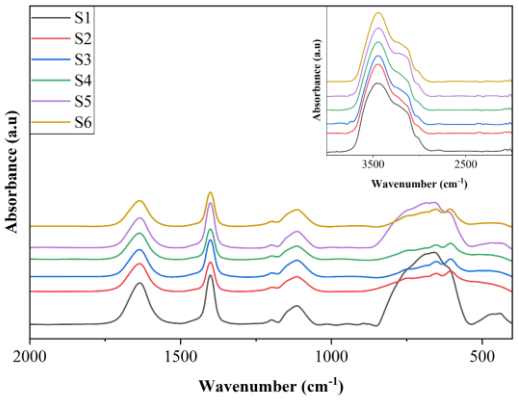

Fig. 2: FTIR absorption spectra of (60-x-y) TeO_2 – 40 ZnO – x Sb_2O_3 – y Er_2O_3 glass series at various compositions from 2000 – 400 cm^{-1}, and the inset is the same FTIR spectra from 4000 – 2000 cm^{-1}.

5.2 Fourier Transform Infrared (FTIR)

Fig. 2 shows the FTIR spectra of (60-x-y) TeO_2 – 40 ZnO – x Sb_2O_3 – y Er_2O_3 glass series, where x and y were varied in the range of $0 < x < 1.0$ mol% and $0 < y < 5.0$ mol%, given in Table 1. All spectra exhibit several characteristic absorption features within the 400 – 4000 cm^{-1} range, as shown in the inset graph in Fig. 2, indicating the presence of various vibrational modes in the glass structure. A broad absorption band appears in the region of 3100 – 3700 cm^{-1} for all spectra, typically attributed to the stretching vibration of the OH group [16], [17]. The presence of this group suggests that there might be water content or moisture trapped during the grounding process of the glass powder and KBr. There is a broad absorption peak around ~1650 cm^{-1} that appears for all samples, which is related to the bending vibration of OH bonds [17], [18], [19]. There is a sharp absorption band centred at ~1400 cm^{-1} detected for all samples, which is unusual for ZnO-TeO_2-based glass. Usually, this band is assigned to the carbonate (CO_3^{2-}) or nitrate (NO_3^{2-}) impurities [20]. This band might arise due to the atmospheric CO_2 during the preparation of KBr pellet. Nevertheless, the persistence of this band across all compositions also raises the possibility of a new bonding environment related to zinc tellurite glass, which would require complementary techniques such as Raman spectroscopy or nuclear magnetic resonance (NMR) to confirm it. There is also an absorption peak detected at ~1120 cm^{-1} with a shoulder at ~1193 cm^{-1} attributed to the Te-O-Zn linkages [17], [21]. These peaks seem not to be affected by the change in the compositions. On top of that, several prominent bands appear in the region 1000 – 400 cm^{-1}. All samples exhibit a broad absorption band that spans between 400 – 800 cm^{-1}. The observed broadening of the bands can be either from the overlapping of some individual bands or the distribution of the bond angles, the bond lengths, and the fluctuations of the local electronic and atomic environments in the amorphous state [22]. Therefore, it is necessary to carry out the deconvolution to separate those peaks. The deconvolution was carried out using Gaussian function, and the parameters such as the peak centre (C) and the relative area of the band (A) were recorded in Table 2, and the deconvolution of the spectra is shown in Fig. 3.

As seen in the deconvolution data and spectra in Table 2 and Fig. 3, all six samples exhibit a common absorption feature that spans the region from approximately 400 cm^{-1} to 900 cm^{-1}. This broad absorption is an envelope of seven absorption bands, representing the vibration modes of Te-O and Zn-O. Table 3 shows the band assignments of the functional group for TeO_2 glass. At low concentration of modifiers (x + y < 3.0 mol%), as observed in S1, S5, and S6, a strong absorption band dominates in the region 690 – 700 cm^{-1}, indicating that the glass network in these samples is primarily composed of TeO_3 structural units. This is mainly due to the high concentration of ZnO, which breaks down the bridging oxygens of TeO_2 glass network (Te-O-Te) to form the NBOs, which reduces the formation of TeO_4 units and creates more TeO_3 units [23], [24]. Upon the inclusion of modifiers, several peak centres show variations, indicating the structural modification of the zinc tellurite glass network. When the total modifier contents exceed 3.0 mol% (x + y > 3.0 mol%), the band centred at ~430 cm^{-1}, related to the stretching vibration of Zn-O or bending vibration of Te-O-Te linkages [14], [25], [26], gradually diminishes and shifts toward higher wavenumber, around ~460 cm^{-1}. This behaviour may relate to the decrease of Zn-O bonds in the glass, which agrees with the literature [26]. Similarly, the band at ~470 cm^{-1}, also assigned to Te-O-Te linkages, shifts to a higher wavenumber, around ~550 cm^{-1}, suggesting the transformation of weaker bending vibrations of Te-O-Te linkages into

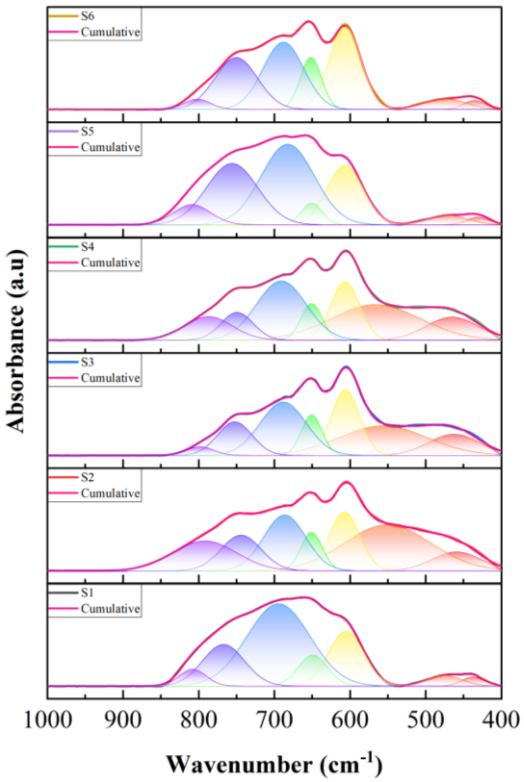

Fig. 3: The deconvolution of FTIR spectra in the region 400 – 1000 cm^{-1} for all samples.

TABLE 2: The deconvolution parameters of FTIR spectra of (60.0 − x − y) TeO_2 – 40.0 ZnO – x Sb_2O_3 – y Er_2O_3 glass in the region 400 – 1000 cm^{-1}, where C is the centre of deconvoluted band (cm^{-1}) and A is the relative area fraction of deconvoluted band (%).

Sample	Molar percentage (mol%)		The centre of deconvoluted band, C (cm^{-1}) and the relative area fraction of deconvoluted band, A (%).							
S1	x = 0	C	437	475	-	605	649	694	767	808
	y = 3.0	A	1.90	3.43	-	18.09	8.52	47.72	16.18	4.16
S2	x = 0	C	-	459	550	607	651	686	744	792
	y = 5.0	A	-	6.70	30.04	13.74	6.31	17.88	10.89	14.43
S3	x = 0.5	C	-	462	556	606	651	688	752	798
	y = 3.0	A	-	10.25	25.37	18.24	8.18	24.21	11.48	2.27
S4	x = 1.0	C	-	465	566	606	651	691	749	787
	y = 3.0	A	-	9.90	26.88	14.35	6.53	25.11	7.64	9.60
S5	x = 0.5	C	431	471	-	607	650	682	756	809
	y = 0	A	1.46	3.32	-	19.18	3.97	37.75	27.73	6.58
S6	x = 0.5	C	436	474	-	606	652	688	750	802
	y = 1.5	A	1.99	4.66	-	27.38	11.47	28.65	23.04	2.80

Table 1: FTIR band assignment in the spectra of TeO_2 glass.

Wavenumber (cm^{-1})	Assignment	Reference
430 – 470	The bending vibration from Te-O-Te or O-Te-O linkages or the stretching vibration of Zn-O in ZnO_4 tetrahedra.	[14], [25], [26]
545 – 590	The stretching vibrations of Te-O-Te bond between TeO_4 and bridging oxygen.	[26], [27]
600 – 650	The stretching vibration of Te-O in TeO_4 tbp.	[15], [28]
650 – 700	The stretching vibration of Te-O in TeO_3 tp.	[15], [24]
740 – 770	The vibration modes of TeO_3 tp or distorted TeO_{3+1}.	[4], [34], [35]
780 – 810	The stretching mode of Te-O with non-bridging oxygen.	[27], [36]

stronger stretching vibrations associated with Te-O-Te bonds involving BO in TeO_4 units [26], [27]. Meanwhile, the bands at ~600 – 650 cm^{-1} that relate to TeO_4 tbp structure remain nearly unchanged for all samples [15], [28]. It is implied that this specific vibrational mode is less affected by the modifiers. However, it is worth noting that these bands appear as a partially overlapped doublet at low concentration of modifiers. Upon the addition of Er_2O_3 and/or Sb_2O_3, the two centres at ~600 cm^{-1} and ~650 cm^{-1} become more widely separated, implying the changed in local environment of Te atoms. The modifiers like Sb_2O_3 and Er_2O_3 can distort the TeO_4 unit, which could alter its bond lengths and angles, thus leading to the splitting of the vibrational modes and the appearance of two distinct peaks in the FTIR [29]. On the other hand, in the region 650 – 800 cm^{-1} corresponding to TeO_3 tp units, the peak centres exhibit significant shifts compared to the nearly unchanged bands at 600 – 650 cm^{-1}, indicating that TeO_3 units are more sensitive to structural modification from the inclusion of Sb_2O_3 and Er_2O_3. This behaviour might suggest that Sb_2O_3 and Er_2O_3 may have alter the bond lengths and angles from TeO_3 unit more than from TeO_4 unit, which explained the shift of peak centres.

To evaluate the effect of Sb_2O_3 and Er_2O_3 on the formation of BO and NBO in $ZnO\text{-}TeO_2$ glass, the relative fraction area of the deconvoluted band (A) can be used, as it reflects the concentration of the structural unit associated with each peak centre. The relations in (1) and (2) can be used to evaluate the concentration of TeO_4 and TeO_3 units [30]:

$$P_{TeO4} = \frac{A_{TeO4}}{A_{TeO4} + A_{TeO3}} \times 100\% \quad (1)$$

$$P_{TeO3} = \frac{A_{TeO3}}{A_{TeO4} + A_{TeO3}} \times 100\% \quad (2)$$

where P_{TeO4} and P_{TeO3} refers to the percentage fraction area of TeO_4 and TeO_3 unit, while A_{TeO4} and A_{TeO3} is the collective area of TeO_4 and TeO_3 unit, respectively. These relations can be used to evaluate the presence of BO and NBO in $ZnO\text{-}TeO_2$,

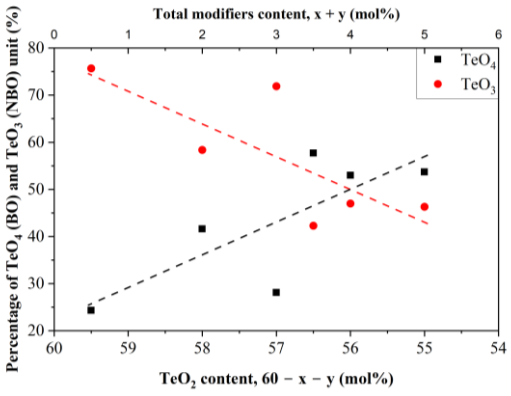

Fig. 4: Variation of TeO_4 and TeO_3 with the concentration of modifiers at the expense of TeO_2. The dashed line represents the trendline of the plot.

since TeO_4 units are typically associated with BOs, while TeO_3 are linked with NBOs. Fig. 4 shows the plot of percentage area for TeO_4 and TeO_3 vs the concentration of TeO_2. Based on Fig. 4, it shows the variation of TeO_4 and TeO_3 units with the decrease of TeO_2 induced by the addition of Sb_2O_3 and Er_2O_3. For S5, S6, and S1, TeO_3 unit is higher than TeO_4, which implied that the content of NBO is high in these samples. The high NBO content is due to the high concentration of ZnO, as discussed above. As the modifiers increase at the expense of TeO_2, the fraction of TeO_3 units decrease while TeO_4 units increase, indicating the creation of BO in the glass network. For S3, S4, and S2, the inclusion of modifiers at the expense of TeO_2 leads to a more balanced ratio of BO and NBO units within the glass network, as reflected in the graph. This is crucial as it will impact the functionality of the glass. Excessive NBOs are known to weaken the network connectivity, which could reduce the overall stability of the glass network [31]. On the contrary, too little NBO could potentially reduce the refractive index of the glass, as the presence of NBO has been correlated with an increase in the refractive index of various glass systems [32], [33]. A glass network that maintains both BO and NBO units in proportion is more likely to combine mechanical durability with favourable optical characteristics, an important quality for glasses intended for photonic applications, where stability and high refractive index must coexist.

6.0 CONCLUSION

In conclusion, a series of ZnO-TeO_2 glasses with a stable glass network have been successfully fabricated by adding Er_2O_3 and Sb_2O_3. The structural properties of the fabricated glasses were characterized using XRD and FTIR spectroscopy. XRD patterns confirmed the amorphous nature of all samples while the FTIR results revealed the absorption bands at 400 – 1000 cm^{-1}, 1120 – 1190 cm^{-1}, 1400 cm^{-1}, 1650 cm^{-1}, and 3100 – 3700 cm^{-1}. To resolve the overlapping bands in the 400 – 1000 cm^{-1}, a deconvolution analysis was performed, which revealed seven distinct absorption bands corresponding to the vibration modes of Te-O and Zn-O. At low concentration of modifiers, the band at ~690 – 700 cm^{-1} appeared as the most intense, indicating the NBO-rich environment in the glass. As the modifiers increased, the intensity of the band decreased, suggesting the reduction in NBO and a transition towards a more balanced distribution of BOs and NBOs.

ACKNOWLEDGEMENTS

The authors would like to express sincere gratitude towards i-CRIM Lab, UKM, and Kulliyyah of Science, IIUM for providing the service analysis of XRD and FTIR used in this study.

REFERENCES

1. S. O. Adeleye, A. A. Adeleke, P. Nzerem, A. I. Olosho, E. N. Anosike-Francis, T. S. Ogedengbe, P. P. Ikubanni, R. A. Saleh, J. A. Okolie. “A Review of the Physical, Optical and Photoluminescence Properties of Rare Earth Ions Doped Glasses,” Trends in Sciences, vol. 21, no. 12, pp. 8759, 2024.
2. P. Vani, G. Vinitha, and N. Manikandan, “Structural, luminescence and nonlinear optical properties of erbium doped barium tellurite glasses for photonic applications,” Journal of Materials Science: Materials in Electronics, vol. 34, no. 1, pp. 1–22, 2023.
3. E. A. Anashkina, “Laser Sources Based on Rare-Earth Ion Doped Tellurite Glass Fibers and Microspheres,” Fibers, vol. 8, no. 5, 2020.
4. Y. Sun, A. Chen, J. Yang, K. Zhang, S. Wang, X. Xu, L. Niu, Y. Jing, C. Wang, L. Ren, J. Zhang, “Net gain in C+L band from LED pumped broadband emission in Er3+-doped oxyhalide tellurite glass,” Ceram Int, vol. 50, no. 11, pp. 18968–18976, 2024.

5. G. Torun, T. Kishi, D. Pugliese, D. Milanese, and Y. Bellouard, "Formation Mechanism of Elemental Te Produced in Tellurite Glass Systems by Femtosecond Laser Irradiation," Advanced Materials, vol. 35, no. 20, p. 2210446, 2023.
6. V. Tomar, R. Pandey, and P. Singh, "Influence of quenching rate and quenching media on formation of TeO2 glasses," Journal of Materials Science: Materials in Electronics, vol. 32, no. 13, pp. 17726–17740, 2021.
7. J. Hrabovsky, L. Strizik, F. Desevedavy, S. Tazlaru, M. Kucera, L. Nowak, R. Krystufek, J. Mistrik, V. Dedic, V. Kopecky Jr, G. Gadret, "Optical, magneto-optical properties and fiber-drawing ability of tellurite glasses in the TeO2–ZnO–BaO ternary system," J Non Cryst Solids, vol. 624, p. 122712, 2024.
8. V. Kozhukharov, H. Bürger, S. Neov, and B. Sidzhimov, "Atomic arrangement of a zinc-tellurite glass," Polyhedron, vol. 5, no. 3, pp. 771–777, 1986.
9. M. Elisa, R. C. Stefan, I. C. Vasiliu, S. M. Iordache, A. M. Iordache, B. A. Sava, L. Boroica, M. C. Dinca, A. V. Filip, A. C. Galca, C. Bartha, "A New Zinc Phosphate-Tellurite Glass for Magneto-Optical Applications," Nanomaterials, vol. 10, no. 9, pp. 1875, 2020.
10. M. K. Halimah, A. A. Awshah, A. M. Hamza, K. T. Chan, S. A. Umar, and S. H. Alazoumi, "Effect of neodymium nanoparticles on optical properties of zinc tellurite glass system," Journal of Materials Science: Materials in Electronics, vol. 31, no. 5, pp. 3785–3794, 2020.
11. G. Jagannath, B. Eraiah, A. Gaddam, H. Fernandes, D. Brazete, K. Jayanthi, K. N. Krishnakanth, S. Venugopal Rao, J. M. Ferreira, K. Annapurna, A. R. Allu, "Structural and Femtosecond Third-Order Nonlinear Optical Properties of Sodium Borate Oxide Glasses: Effect of Antimony," Journal of Physical Chemistry C, vol. 123, no. 9, pp. 5591–5602, 2019.
12. Y. Hordieiev and A. Zaichuk, "Structural, thermal, and radiation shielding properties of antimony-doped zinc borate glasses," Sci Rep, vol. 15, no. 1, pp. 1–12, 2025.
13. M. Hongisto, A. Veber, Y. Petit, T. Cardinal, S. Danto, V. Jubera, L. Petit, "Radiation-Induced Defects and Effects in Germanate and Tellurite Glasses," Materials, vol. 13, pp. 3846, 2020.
14. N. R. Mohamad Azaludin and N. S. Sabri, "Infrared spectroscopy of mixed glass former effect in borotellurite glasses: A review," Gading Journal of Science and Technology, vol. 4, no. 1, pp. 94–102, 2021.
15. S. N. Nazrin, M. S. Sutrisno, H. B. Zaman, N. Jothi, A. Assaiqeli, and S. Ezzine, "Enhanced photoluminescence and optical properties of erbium-doped zinc tellurite glasses for visible and near-infrared photonic applications," J Lumin, vol. 281, pp. 121184, 2025.
16. P. Naresh, B. Kavitha, H. K. Inamdar, D. Sreenivasu, N. Narsimlu, C. Srinivas, V. Sathe, K. S. Kumar, "Modifier role of ZnO on the structural and transport properties of lithium boro tellurite glasses," J Non Cryst Solids, vol. 514, pp. 35–45, 2019.
17. S. K. Ghoshal, A. Awang, M. R. Sahar, and R. J. Amjad, "Spectroscopic and structural properties of TeO2-ZnO-Na2OEr2O3-Au glasses," Chalcogenide Letters, vol. 10, no. 10, pp. 411–420, 2013.
18. Y. B. Saddeek, "Network structure of molybdenum lead phosphate glasses: Infrared spectra and constants of elasticity," Physica B Condens Matter, vol. 406, no. 3, pp. 562–566, 2011.
19. M. Reza Dousti, M. R. Sahar, S. K. Ghoshal, R. J. Amjad, and A. R. Samavati, "Effect of AgCl on spectroscopic properties of erbium doped zinc tellurite glass," J Mol Struct, vol. 1035, pp. 6–12, 2013.

20. D. S. Volkov, O. B. Rogova, and M. A. Proskurnin, "Organic matter and mineral composition of silicate soils: FTIR comparison study by photoacoustic, diffuse reflectance, and attenuated total reflection modalities," Agronomy, vol. 11, no. 9, p. 1879, 2021.
21. M. R. Sahar, K. Sulhadi, and M. S. Rohani, "Spectroscopic studies of TeO2-ZnO-Er2O3 glass system," J Mater Sci, vol. 42, no. 3, pp. 824–827, 2007.
22. Y. B. Saddeek and N. Z. Elsayed, "Structural and mechanical features of some lanthanum tellurite glasses," Can J Phys, vol. 93, no. 4, pp. 460–465, 2015.
23. S. N. Nazrin, M. K. Halimah, and F. D. Muhammad, "Comparison study of optical properties on erbium-doped and silver-doped zinc tellurite glass system for non-linear application," Journal of Materials Science: Materials in Electronics, vol. 30, no. 7, pp. 6378–6389, 2019.
24. H. A. A. Sidek, S. Rosmawati, Z. A. Talib, M. K. Halimah, and W. M. Daud, "Synthesis and optical properties of ZnO-TeO 2 glass system," Am J Appl Sci, vol. 6, no. 8, pp. 1489, 2009.
25. S. K. Ahmmad, M. A. Samee, S. M. Taqiullah, and S. Rahman, "FT-IR and Raman spectroscopic studies of ZnF2–ZnO–As2O3–TeO2 glasses," Journal of Taibah University for Science, vol. 10, no. 3, pp. 329–339, 2016.
26. D. E. Fausta, A. Marzuki, and Cari, "Infrared absorption spectra analysis of TeO2-ZnO-Bi2O3-TiO2 doped B2O3 glasses," J Phys Conf Ser, vol. 1511, no. 1, p. 012076, 2020.
27. A. Azuraida, M. K. Halimah, M. Ishak, L. Hasnimulyati, and S. I. Ahmad, "GAMMA RAY SHIELDING PARAMETER OF BARIUM-BORO-TELLURITE GLASS," Chalcogenide Letters, vol. 17, no. 4, pp. 187–196, 2020.
28. R. Stefan, M. Karabulut, A. Popa, E. Culea, L. Bolundut, L. Olar, P. Pascuta, "A spectroscopic study of the influence of CuO addition on the ZnO-TeO2 glass and glass ceramics," J Non Cryst Solids, vol. 498, pp. 430–436, 2018.
29. L. Brand, V. Anjos, and M. J. V. Bell, "Optical and structural analysis of tellurite matrices with different modifiers," Opt Mater (Amst), vol. 138, pp. 113470, 2023.
30. Y. S. Rammah, N. A. M. Alsaif, Z. Y. Khattari, M. S. Shams, R. A. Elsad, and M. S. Sadeq, "Synthesis, physical, FTIR, and optical characteristics of B2O3·CaO·ZnO glasses doped with Nb2O5 oxide: Experimental investigation," Journal of Materials Science: Materials in Electronics, vol. 33, no. 30, pp. 23749–23760, 2022.
31. J. E. Shelby, "Introduction to Glass Science and Technology," Introduction to Glass Science and Technology, 2020.
32. A. S. Asyikin, M. K. Halimah, A. A. Latif, M. F. Faznny, and S. N. Nazrin, "Physical, structural and optical properties of bio-silica borotellurite glass system doped with samarium oxide nanoparticles," J Non Cryst Solids, vol. 529, p. 119777, 2020.
33. Y. Zhu et al., "Concentration dependent structural, thermal and luminescence properties in Er3+/Tm3+ doped tellurite glasses," J Non Cryst Solids, vol. 507, pp. 19–29, 2019.
34. H. Elkholy, H. Othman, I. Hager, M. Ibrahim, and D. de Ligny, "Europium-Doped Tellurite Glasses: The Eu2+ Emission in Tellurite, Adjusting Eu2+ and Eu3+ Emissions toward White Light Emission," Materials, vol. 12, no. 24, p. 4140, 2019.
35. N. Elkhoshkhany, S. Y. Marzouk, and S. Shahin, "Synthesis and optical properties of new fluoro-tellurite glass within (TeO2-ZnO-LiF-Nb2O5-NaF) system," J Non Cryst Solids, vol. 472, pp. 39–45, 2017.
36. Y. B. Saddeek, K. A. Aly, K. S. Shaaban, A. M. Ali, M. M. Alqhtani, A.

M. Alshehri, M. A. Sayed, E. A. Wahab EA, “Physical properties of B2O3–TeO2–Bi2O3 glass system,” J Non Cryst Solids, vol. 498, pp. 82–88, 2018.